Regular Article

Single atom spectroscopy with reduced delocalization effect using a 30 kV-STEM

K. Suenaga[a], Y. Iizumi, and T. Okazaki

Nanotube Research Center, National Institute of Advanced Industrial Science and Technology (AIST), Tsukuba 305-8565, Japan

Abstract. Imaging and chemical analysis of individual metallofullerene molecules were successfully carried out without massive destruction using a scanning transmission electron microscope (STEM) operated at 30 kV. Electron energy-loss spectroscopy (EELS) unambiguously identified the constituent atom of each metallofullerene molecule. The profile of EELS chemical map measured across the single atom provides a rough estimate of EELS signal delocalization, which is considerably reduced using accelerating voltage as low as 30 kV.

Element selective single atom imaging was first demonstrated a decade ago [1]. Two major scientific/techno-logical contributions were crucial to realize this experiment: (i) a preparation of a suitable specimen which contains heavy metal atoms far enough apart, the so-called *peapods* [2] and (ii) a fully digitized STEM-EELS system enabling image spectrum – the *Colliex* instrument [3]. Even though a most efficient detector (20 counts per electron at that time) was used to count the number of inelastically scattered electrons, the destruction of molecules was inevitable due to the irradiation damage. A high current dose was required to achieve a high SN ratio to get EELS signals from single atoms with a primary electron energy as high as 100 keV.

Reducing the accelerating voltage of TEM/STEM is becoming essential when one aims to image any beam sensitive objects. Lower accelerating voltage is preferred for observation of small molecules made of light elements, in order to prevent the destruction of the molecular structures by the knock-on effect and, more importantly, to enhance the image/EELS contrast. In order to compensate for the loss of spatial resolution, more sophisticated electron optics are definitely required to reduce the residual geometric/chromatic aberrations of the TEM/STEM [4].

Sawada et al. designed a new type of Cs corrector with triple dodecapole elements (DELTA system) to reduce the six-fold astigmatism [5,6]. Correction of higher order aberration is very useful for a TEM/STEM operated at low accelerating voltages. Nowadays JEOL 2100F equipped with the DELTA corrector shows the world's best performance in terms of the spatial resolution normalized by the wavelength, as it was shown by observing the Si (2 2 4) lattice

(111 pm) which corresponds to 16 times of the wavelength at 30 kV ($\lambda = 7$ pm) [7].

One of the major advantages of low voltage STEM was demonstrated by chemical analysis of individual molecules without massive structural destruction [8]. However even at 60 kV, high dose observation also showed significant irradiation damage on metallofullerene molecules, as proved by the release of the encaged atoms [9]. This effect has already been predicted by a simple calculation of the knock-on threshold energy based on the estimated displacement energy (E_d) [10]. Figure 1 shows the calculated knock-on threshold energies for carbon materials with various shapes of atom packing. It suggests that a 60 kV accelerating voltage cannot be low enough to entirely avoid irradiation damage in fullerenes which have a very high curvature and about 35 kV or less will be indeed preferred to observe this kind of molecules.

We show here that single atom spectroscopy can be conducted with hardly noticeable irradiation damage by reducing the accelerating voltage down to 30 kV. We have used a GIF Quantum spectrometer (Gatan) specially modified for low voltage observation [11].

Figure 2 shows a comparison of STEM-ADF images of Er@C_{82} peapods. Their specimen preparation procedure was described elsewhere [8]. It can be clearly seen in Figure 2b that the Er@C_{82} metallofullerenes have coalesced and punctured allowing the Er atoms, which appear as bright dots, to escape from their fullerene cage and travel along the single wall nanotube (SWNT) during ADF observation at 60 kV. In contrast, the Er@C_{82} metallofullerene molecules observed at 30 kV (Fig. 2a) mostly retain an intact structure and carry single Er atom in each cage. This is an evidence that the fullerene cage structure cannot be easily punctured with an incident electron beam at 30 kV. Even if we consider the lower beam current
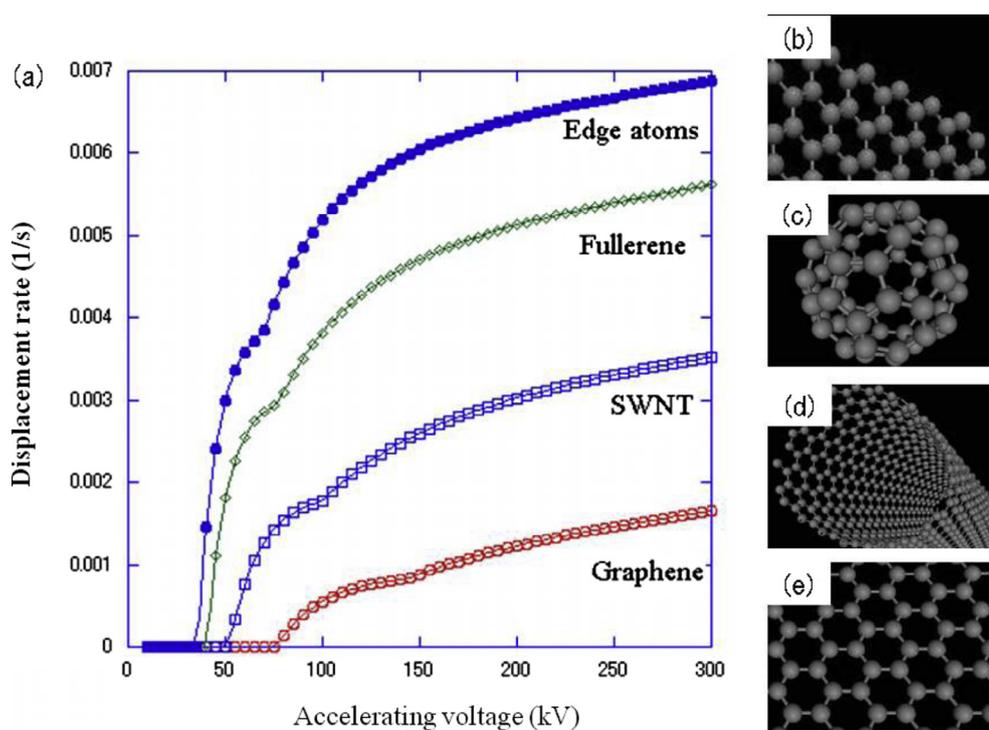
a e-mail: suenaga-kazu@aist.go.jp

Fig. 1. (Color online) (a) Estimated knock-on threshold energies for various carbon materials with different configuration. Displacement energies (E_d) previously reported [10] were used for calculations. (b) Accelerating voltages less than 35 kV are indeed preferred for observing the graphene edge atoms and (c) the fullerene molecules, while the carbon nanotube and graphene bulk structures are more resistant up to (d) 50 and (e) 80 kV respectively.
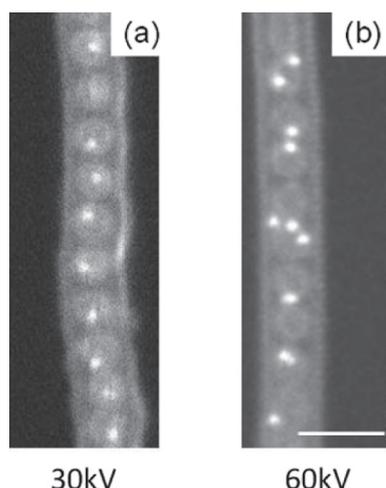

Fig. 2. STEM-ADF images showing the different degree of irradiation damages in metallofullerene peapods (Er@C_{82} encapsulated in SWNT) during STEM observation at 30 and 60 kV ((a) and (b), respectively) [7]. Most of the metallofullerene molecules are punctured or coalesced due to the irradiation damage in the image taken at 60 kV, while they do not show massive irradiation damage and their cage structure is intact at 30 kV. Scale bar = 2 nm.

density at 30 kV, the damage threshold of primary beam energy must certainly lie between 30 and 60 kV. This is consistent with the prediction above which estimated the damage threshold to be about 35 kV. Note that the non-straight wall of SWNT seen in Figure 2a is an effect of the pre-treatment for specimen cleaning and is not considered in this discussion on irradiation damage of fullerene molecules.

We then analyzed a mixed peapod with two or more different metallofullerenes. M@C_{82} (M = La, Ce, or Er) molecules were chosen and co-doped inside SWNTs. The ADF image clearly shows the molecular structures encapsulated inside the SWNT (Fig. 3a). Each of the two metallofullerene molecules in the indicated rectangle area carries one metal atom which has a brighter contrast. Although the ADF image does not provide elemental information on these two atoms, we can identify them by EELS. Figure 3b shows the EELS spectra recorded on the two atoms seen in Figure 3a. The EELS spectrum in green corresponds to the atom indicated by green arrow. It is the sum of four spectra, each of which was acquired for 0.05 s. The SN ratio is high enough to extract the La N-edge. On the other hand, the atom indicated by blue arrow is assigned to Ce and its peak position ($\sim$122 eV) fits very well that of Ce^{3+} [8]. The metallofullerene structure is not completely stable even under the 30 kV incident probe. If the puncturing of the cages had hardly ever been observed, longer acquisition time often leads to movements of the metal atoms inside their cage.

Although the two edges of La N and Ce N severely overlap, we could identify the elements (La: $Z = 57$ and
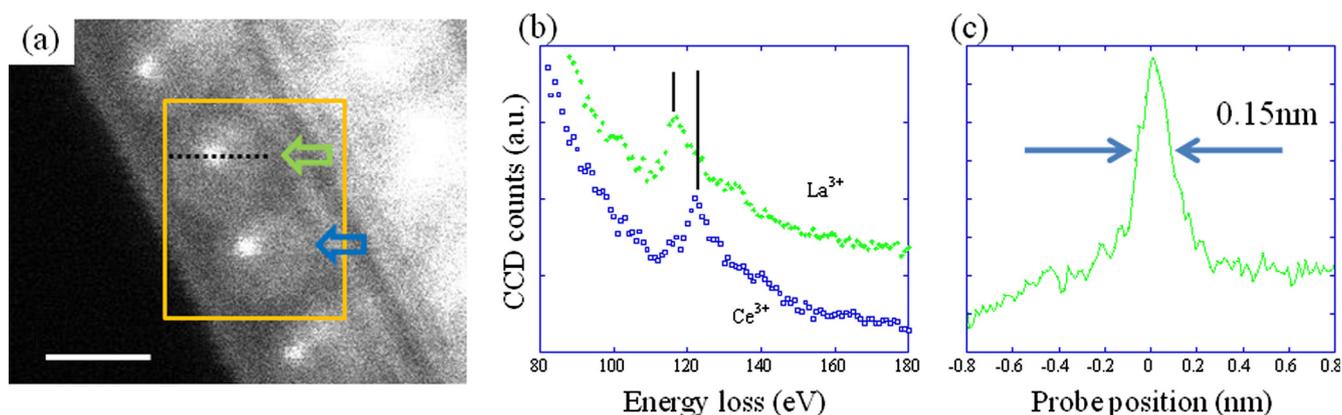
Fig. 3. (Color online) Detailed analysis of the mixed peapods (La@C$_{82}$ and Ce@C$_{82}$). (a) The rectangle in this ADF image shows the area where the spectrum images of Figure 4 were acquired. (b) EELS spectra recorded from the two metal atoms indicated in (a). The atom indicated by a green arrow was identified as La and the blue one as Ce. (c) Intensity profile across the ADF image of a La atom corresponding to the dotted line in (a). The FWHM is roughly estimated as 0.15 nm, which reflects the probe size as well as possible atom movement or vibration.
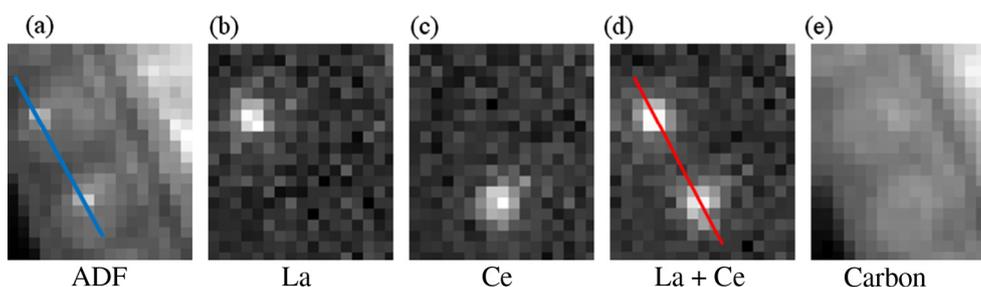

Fig. 4. (Color online) Spectrum images obtained at the indicated rectangle in Figure 3a. 17×20 EELS spectra were recorded with a 0.11 nm probe step and 0.05 s acquisition time. The energy dispersion was set to 0.25 eV/channel and two channel binning was applied to minimize the readout time. (a) ADF image obtained simultaneously with EELS maps. (b,c) Chemical maps for La and Ce N-edges after the standard MLLS fitting. (d) La + Ce map. (e) EELS chemical map of carbon K-edge.

Ce: $Z = 58$) of two encaged atoms as well as the oxidation state of Ce atom (Ce^{3+}). This result confirms the previous experiment that was performed at 60 kV primary energy [8]. Figure 3b shows the profile of ADF counts across the atom indicated by green arrow. The FWHM of the ADF profile of single atoms is about 0.15 nm, which should reflect the probe size at 60 kV possibly broadened by some atom movement or vibration.

The results of spectrum image performed on the rectangle in Figure 3a are summarized in Figure 4. They were recorded with 0.11 nm constant steps and 0.05 s acquisition time for each. The background was removed to extract the EELS La and Ce N-edges using the multiple linear least square (MLLS) fitting from the Digital Micrograph package (Gatan Inc.), which is perfectly suited to get independently the La and Ce signals.

The ADF image (a) was simultaneously recorded at each pixel point during the spectrum image, therefore the positions of two metal atoms in the ADF image should perfectly match to those in EELS maps. The La and Ce maps after the MLLS fitting are shown in Figures 4b and 4c, respectively. In order to better compare the size of atoms in EELS chemical maps, a La + Ce map is also added in Figure 4d. Figure 4e shows the carbon K-edge map which was also simultaneously obtained.

Figure 5 shows the intensity profiles of ADF and EELS along the blue and red lines in Figures 4a and 4d respectively. The number of pixel points is arguably small but we can roughly estimate the effect of EELS signal delocalization by comparing the two profiles. The two maxima in EELS map clearly correspond to those for La and Ce atoms in the ADF image. The FWHM of the two peaks in EELS map can be simply measured around 0.33–0.35 nm, whereas the ADF profile apparently shows a slightly smaller FWHM (0.15–0.20 nm). The delocalization effect measured by the difference of two profiles could be extremely small. Note that the FWHM may not be a good measure of EELS signal delocalization because the delocalization is supposed to add large tails to the profile. Further experiments with higher data points will be anticipated to corroborate the present results for future.

Within the classical theory, the degree of delocalization (a typical $1/e$ decrease in the intensity) can be estimated to be equal to $v/\Delta E$, where v is the speed of electron and ΔE the energy loss. We can therefore expect it as 0.3 nm for carbon K-edge (300 eV) and 0.6 nm for La and Ce N-edges (150 eV) when the primary energy of incident electron is 100 kV [12]. This value for delocalization is correspondingly reduced for 30 kV electrons to about
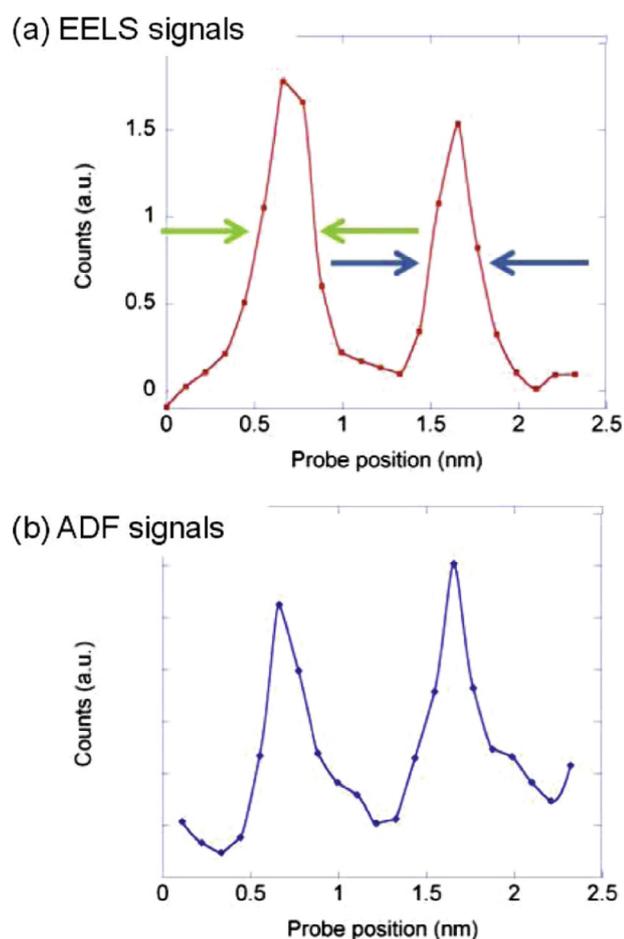
(a) EELS signals

(b) ADF signals

Fig. 5. (Color online) (a) Profile of EELS La and Ce *N*-edges intensities obtained across the two atoms indicated by the red line in Figure 4d. (b) ADF profile along the blue line in Figure 4a. In spite of the low number of data points, the FWHM of each atom profile in EELS chemical map of La and Ce *N*-edges can be roughly estimated around 0.33–0.35 nm that is slightly larger than for their ADF signals. Note that the ADF profile involves small bumps or shoulders due to the contrast of fullerene cages at the right side of two metal atoms.

0.33 nm ($= 0.6 \times (30/100)^{1/2}$) for the La and Ce *N*-edges. This value seems consistent with the experimental results if the small amount of data point and the size of incident probe are considered.

In summary, we would like to emphasize in this paper the advantages of the low voltage STEM in three different aspects, namely (i) less knock-on damage, (ii) higher ADF/EELS contrast, and (iii) less pronounced delocalization effect. The real merit of low voltage STEM may lie in the third. Even though smaller probes can be obtained with higher accelerating voltage, the delocalization effect will become more and more important. One should optimize the accelerating voltage for each experiment depending on the specific energy loss of the target element and the inter-atomic distance to resolve.

References

1. K. Suenaga et al., Science **290**, 2280 (2000)
2. K. Hirahara et al., Phys. Rev. Lett. **85**, 5384 (2000)
3. M. Tencé, M. Quartuccio, C. Colliex, Ultramicroscopy **58**, 42 (1995)
4. See the Triple C project website, http://www.busshitu.jst.go.jp/en/kadai/year03/team03.html
5. H. Sawada et al., J. Electron Microsc. **58**, 341 (2009)
6. H. Sawada et al., Ultramicroscopy **110**, 958 (2010)
7. T. Sasaki et al., J. Electron Microsc. **59**, S7 (2010)
8. K. Suenaga et al., Nat. Chem. **1**, 415 (2010)
9. O. Krivanek et al., Ultramicroscopy **110**, 935 (2010)
10. F. Banhart, Rep. Prog. Phys. **62**, 1181 (1999)
11. A. Gubbens et al., Ultramicroscopy **110**, 962 (2010)
12. A. Howie, in *Presentations at Past, Present and Future of (S)TEM and its Application, Paris, France, 2010*